Zygote **14** (February), pp. 23–32. © 2006 Cambridge University Press
doi:10.1017/S0967199405003503 Printed in the United Kingdom

Peptide-induced hyperactivation-like vigorous flagellar movement in starfish sperm

Kogiku Shiba[1], *Tomoko Tagata*[2], *Junko Ohmuro*[1], *Yoshihiro Mogami*[2], *Midori Matsumoto*[3], *Motonori Hoshi*[3] *and Shoji A. Baba*[1]

Ochanomizu University, Tokyo, and Keio University, Yokohama, Japan

Date submitted: 17.05.05 Date accepted: 30.08.05

Summary

Asterosap, a sperm-activating peptide (SAP) from the starfish egg jelly coat, is diffusible and controls a cGMP-signalling pathway in starfish sperm in the same manner as resact, a potent chemoattracting SAP in sea urchins. This fact suggests that asterosap may serve as a chemoattractant like resact at concentrations with appropriate gradients. Since asterosap is one of three egg jelly components, which in concert induce the acrosome reaction, it is still worthwhile to evaluate how asterosap modulates sperm motility prior to this reaction. We analysed the flagellar movement of sperm of the starfish *Aphelasterias japonica* in artificial seawater (ASW) containing the asterosap isoform P15 at 1 μmol l^{-1}. We found that sperm swim straighter with more symmetrical flagellar movement in P15 than in ASW, but without any significant difference in the flagellar beat frequency and the swimming velocity. The flagellar movement is, however, dramatically different between sperm firmly attached to the solid surface by the head in P15 and those attached in ASW: in P15 the flagellum bends to a greater extent, with higher curvature and with higher shear angle up to a right angle to the flagellar wave axis, and beats at an increased frequency. The vigorous flagellar movement of sperm, which can be activated when sperm are placed in high-load circumstances just as entering into a jelly layer, may increase propulsive forces and hydrodynamic resistances, allowing sperm to undergo the acrosome reaction as effectively as possible.

Keywords: Acrosome reaction, *Aphelasterias japonica*, Asterosap, Flagella, Starfish sperm

Introduction

J.C. Dan discovered the acrosome reaction in sea urchins (Dan, 1952), starfish (Dan, 1954) and later in several other marine invertebrates (Hoshi *et al*., 1994). In these species, spermatozoa react to species-specific egg water by undergoing this reaction (Dan, 1952, 1954). To induce the acrosome reaction in starfishes, three egg jelly components in concert act on spermatozoa: a species-specific glycoprotein named acrosome reaction-inducing substance (ARIS), a group of sulfated steroidal sappiness named Co-ARIS, and sperm activating peptides (SAPs) (Hoshi *et al*., 1994). Twelve SAPs were purified and structurally identified from the starfish *Asterias amurensis*, and they were collectively named asterosaps (Nishigaki *et al*., 1996). These SAPs are specific in inducing the acrosome reaction in a group of starfish species including *Asterias amurensis* and *Aphelasterias japonica* (Matsumoto *et al*., 2000).

Asterosap raises the intracellular pH of spermatozoa (Hoshi *et al*., 1994), increases motility of those immotile in slightly acidified artificial seawater (ASW) (Nishigaki *et al*., 1996) and has receptors exclusively on the flagellum (Nishigaki *et al*., 2000). An NH_2-terminal partial sequence of the 13 kDa sperm chemoattractant from the starfish *Pycnopodia helianthoides* shows high homology with asterosap (Miller & Vogt, 1996; Matsumoto *et al*., 1999), suggesting asterosap is a potent

All correspondence to: Dr Shoji A. Baba, Department of Advanced Biosciences, Graduate School of Humanities and Sciences, Ochanomizu University, 2-1-1 Otsuka, Tokyo 112-8610, Japan. Tel: +81 (03) 59785714. Fax: +81 (03) 59785368. e-mail: baba@cc.ocha.ac.jp
[1]Department of Advanced Biosciences, Graduate School of Humanities and Sciences, Ochanomizu University, 2-1-1 Otsuka, Tokyo 112-8610, Japan.
[2]Department of Biology, Ochanomizu University, Otsuka 2-1-1, Tokyo 112-8610, Japan.
[3]Department of Biosciences and Informatics, Keio University, 3-14-1 Hiyoshi, Kohoku-ku, Yokohama 223-8522, Japan.

https://doi.org/10.1017/S0967199405003503 Published online by Cambridge University Press

chemoattractant (Darszon *et al*., 1999). This hypothesis has been supported by the fact that asterosap controls a cGMP-signalling pathway in starfish sperm in the same manner as resact, a potent chemoattracting SAP in sea urchins (Kaupp *et al*., 2003; Matsumoto *et al*., 2003). It has been reported that *Asterias* sperm respond to asterosap with tumbling episodes and swimming in narrow circles when the hydrolysis of cyclic nucleotides is prevented by preincubation of sperm with IBMX (Matsumoto *et al*., 2003). Recently the chemoattracting activity of and chemotactic motor response to asterosap have been observed in normal seawater (Böhmer *et al*., 2005). There are a good number of SAPs and a variety of chemicals which show a definite chemoattracting activity by appropriate assay methods, and convincing models of sperm chemotaxis have been proposed based on motor responses of sperm in normal seawater containing these substances at concentrations with or without gradients (Eisenbach, 1999; Cook *et al*., 1994; Cosson *et al*., 1984; Ishikawa *et al*., 2004; Kaupp *et al*., 2003; Riffell *et al*., 2002, 2004; Ward *et al*., 1985; Yoshida *et al*., 2003).

Anti-asterosap rabbit IgG neutralizes the ability of the acrosome reaction, and the addition of excess asterosap recovered the neutralization (Nishigaki *et al*., 1996); thus, in seawater, asterosap is important for this reaction. It is therefore interesting to evaluate how asterosap modulates sperm motility prior to the acrosome reaction. In the present paper, we will describe a load-dependent vigorous flagellar movement (hyperactivation) of sperm of the starfish *Aphelasterias japonica* in ASW containing the asterosap isoform P15 from *Asterias amurensis* at concentrations as high as found in regions near the egg. The vigorous flagellar movement of sperm, with the flagellar shaft being vertical to the axis of propulsion, should increase propulsive forces and hydrodynamic resistances, allowing sperm to perform the acrosome reaction as effectively as possible.

Materials and methods

Dry sperm

Sperm was obtained 'dry' from the starfish *Aphelasterias japonica* by cutting the testes. The dry sperm was stored in a refrigerator until used.

Solutions

Artificial seawater (ASW) consisted of 450 mM NaCl, 10 mM KCl, 10 mM $CaCl_2$, 25 mM $MgCl_2$, 28 mM $MgSO_4$, 10 mM Tris-HCl (pH 8.0). The synthetic asterosap isoform P15 (GQTQFGVC*IARVRQQHQGQ-DEASIFQAILSQC*QS, intramolecular disulfide bond between two C*) was used (Matsumoto *et al*., 2003; Nishigaki *et al*., 1996, 2000). The P15 was added into ASW to a final concentration of 0.6 or 1 μmol l^{-1} in preliminary experiments, in which there were qualitatively similar differences between sperm in ASW and those in ASW containing P15. We quantitatively analysed data obtained exclusively from experiments using sperm in ASW containing 1 μmol l^{-1} P15.

Recording and analysis

Dry sperm was diluted about 10^3-fold in ASW or in P15. The sperm suspension was immediately put in an observation chamber made of slide and cover glasses separated with 0.5-mm-thick silicone rubber cut into a rectangular frame. All observations and recordings of sperm movements were performed within 15 min after dilution. Pictures of sperm swimming just under the cover glass and those of sperm attached by the head to the cover glass were recorded at room temperatures through an Olympus phase contrast microscope with a ×40 objective (BH2 with NH40) using a video tape recorder (VTR, Sony DHR-1000, Sony, Tokyo) or a high-speed video recorder (HSVTR, EktaPro HR1000, Kodak, Tokyo) under illumination with a power xenon flash tube driven by laboratory-made power controllers (Baba & Mogami, 1987; Miyake *et al*., 1998). Some of sperm that attached by the head to the cover glass pivoted around the point of attachment. We removed all data of these loosely attached sperm from those to be analysed because the flagellar movement of sperm is known to largely depend on whether they can rotate around the point of attachment (Brokaw & Gibbons, 1975). We refer below to these sperm selected for analysis because of firmness of attachment simply as 'attached'.

Individual frames captured through an image processor (DVworks, I-O Data, Tokyo) from the VTR or HSVTR were treated on a PC using cell motility analysis software, Bohboh (BohbohSoft, Tokyo; Shiba *et al*., 2002, 2005; Ohmuro *et al*., 2004). Using this software the sperm head image could be tracked automatically giving the swimming velocities measured either along the zigzag trajectory made during flagellar beating cycles (trajectory swimming velocity) or along the circular path obtained by smoothing out the zigzag fluctuation (curvilinear swimming velocity). The path curvature, Γ, that is, the reciprocal of the radius of curvature, ρ, of the circular swimming path, was also determined on Bohboh.

Individual images of the flagellum of sperm were also analysed on Bohboh, based on automatic tracking using a modified algorithm of Baba & Mogami (1985), which gave about 300 points per flagellum on Cartesian coordinates. To ensure consistency in defining the sign of angle and curvature, we placed the flagellar image

https://doi.org/10.1017/S0967199405003503 Published online by Cambridge University Press

with the principal bend (bend of larger curvature, P bend) to the right and the reverse bend (R bend) to the left when viewed from base to tip. This occasionally required reflection of images around the x-axis, but only in computation of angle and curvature. The angle of the tangent to the flagellar shaft measured with respect to the direction of the axis of sperm head, which will be referred to as shear angle, ϕ, and that with respect to the x-axis (wave axis), ϕ^x, were computed as functions of time t and distance s along the flagellum measured from the base. The angle ϕ is equivalent to ϕ^x for sperm that are firmly attached to the surface by the head, because the axis of the head is fixed relative to the x-axis. Based on the description by Hiramoto & Baba of flagellar bending waves as 'sine-generated' (Hiramoto & Baba, 1978), the shear angle $\phi(s, t)$ was fitted using equations of the form

$$\phi(s,t) = \phi_a(s)\cos\{(S_\phi(s) - 2\pi f t)\} + \phi_b(s) \quad (1)$$

with fixed s and varying t, where f is the beat frequency and $\phi_a(s)$, $S_\phi(s)$ and $\phi_b(s)$ are the amplitude, phase angle and bias of ϕ as functions of s, respectively. The fitting was performed by the method of least squares for arbitrary functions (Bevington & Robinson, 1992) under conditions with $\phi_a(s)$ being of the positive sign. The rate of shear angle change is given by $2\pi f\phi_a(s)$. The phase angle $S_\phi(s)$ was further fitted using equations of the form

$$S_\phi(s) = S_\phi(0) + (2\pi/\lambda_\phi)s \quad (2)$$

with varying s, where λ_ϕ is the wavelength of 'shear angle wave'. The curvature $\gamma(s, t)$ of flagellar bends was also fitted using equations of the form

$$\gamma(s,t) = \gamma_a(s)\cos\{(S_\gamma(s) - 2\pi f t)\} + \gamma_b(s) \quad (3)$$

with fixed s and varying t, where $\gamma_a(s)$, $S_\gamma(s)$ and $\gamma_b(s)$ are the amplitude, phase angle and bias of γ as functions of s, respectively. The sign of $\gamma_a(s)$ is always set positive. The maximum of the P bend at s is given by $\gamma_a(s) + \gamma_b(s)$ and that of the R bend by $\gamma_a(s) - \gamma_b(s)$, provided that the P and R bends are appropriately distinguished. The phase angle $S_\gamma(s)$ was fitted using equations of the form

$$S_\gamma(s) = S_\gamma(0) + (2\pi/\lambda_\gamma)s \quad (4)$$

with varying s, where λ_γ is the wavelength of the 'curvature wave'. The wavelength λ_ϕ of the 'shear angle wave' is generally equal to λ_γ of the 'curvature wave' and hence represents the wavelength λ of the bending wave measured along the flagellum. The propagation velocity along the flagellum is given by λf.

Results

Swimming sperm

Starfish spermatozoa swam along circular paths (Fig. 1A, B) with the head oscillating synchronously with flagellar beating and hence drawing a zigzag trajectory (thick white lines with thin dots) when close to the cover glass, as shown in Fig. 1. There was no significant difference in either trajectory or curvilinear swimming velocity (Table 1), or in the beat frequency, wavelength and propagation velocity of flagellar bending, between sperm in ASW and those in P15 (Tables 1, 2). The radius of curvature, ρ, of the circular swimming path, however, was larger in P15 than in ASW, that is to say, the path curvature, Γ, was lower in P15 (Fig. 1; Table 1). Briefly, sperm in P15 swam along a straighter path, due to more symmetrical flagellar bending, than those in ASW (Fig. 1C, D). There was in fact an apparent difference in the curvature of flagellar bending: a decrease in the P bend over the entire length of flagellum in P15 and an increase in the R bend at the distal region, resulting in more symmetrical bending (Fig. 2).

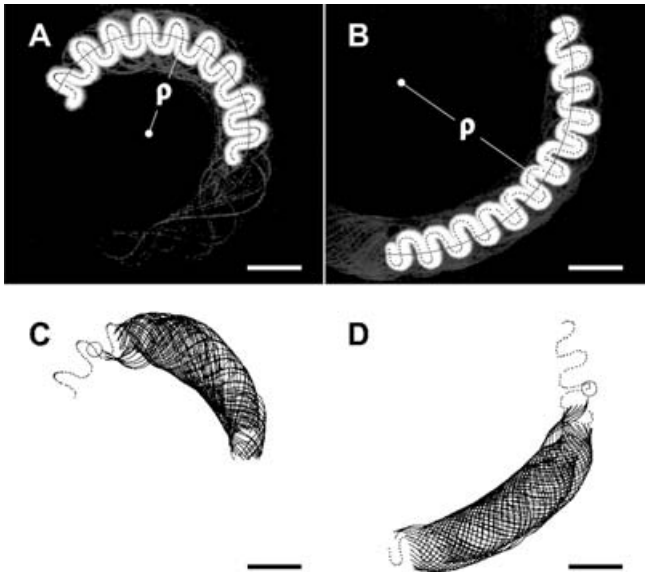


Figure 1 P15-induced changes in swimming of *Aphelasterias japonica* sperm. (*A*), (*B*) The swimming trajectories of one spermatozoon in ASW (*A*) and of another in 1 μmol l^{-1} P15 (*B*) over a period of 0.25 s, both reconstructed from a 1000-fps HSVTR. The radius of curvature (ρ) of the circular swimming path is 18.5 μm (0.054 μm^{-1} in path curvature) in ASW (*A*) and 31.8 μm (0.031 μm^{-1}) in P15 (*B*). The trajectories (thick white lines with thin dots) of the sperm head are constructed respectively by image processing and by auto-tracking on Bohboh. (*C*), (*D*) The flagellar bending forms of these spermatozoa in ASW (*C*) and in P15 (*D*) in about one-and-half beat cycles (50 frames). Scale bars represent 10 μm. Temperature 20 °C.

https://doi.org/10.1017/S0967199405003503 Published online by Cambridge University Press

Table 1 Effects of the asterosap isoform P15 on starfish sperm swimming

	Solution	
	ASW	P15[a]
Beat frequency (Hz)	32.7 ± 6.6 ($N = 100$)	32.5 ± 6.9 ($N = 100$)
Swimming velocity (μm s^{-1})		
Trajectory	375.5 ± 111.4 ($N = 12$)	356.6 ± 152.3 ($N = 11$)
Curvilinear	145.1 ± 51.9 ($N = 12$)	126.3 ± 65.1 ($N = 11$)
Path curvature, Γ(μm^{-1})	0.046 ± 0.018 ($N = 23$)	0.031 ± 0.012 ($N = 20$)**

Values are means ± SD (N is the number of spermatozoa).
[a]The solution P15 is ASW, which contains 1 μmol l^{-1} P15.
**Significant at $p < 0.01$ (Student's t-test).
The beat frequency was measured stroboscopically and the other parameters from the analysis of VTR. Temperature 20 °C.

Table 2 Effects of the asterosap isoform P15 on starfish sperm flagellar bending

	Solution		Mechanical conditions[b]
	ASW	P15[a]	
Beat frequency (Hz)	33.1 ± 6.1 ($N = 6$)	31.7 ± 9.6 ($N = 7$)	Swimming
	26.4 ± 5.2 ($N = 7$)	33.4 ± 10.4 ($N = 8$)	Attached
Curvature (μm^{-1})			
Max P bend	0.19 ± 0.03 ($N = 6$)	0.16 ± 0.02 ($N = 7$)	Swimming
	0.19 ± 0.03 ($N = 7$)	0.27 ± 0.04 ($N = 8$)**	Attached
Max R bend	0.12 ± 0.01 ($N = 6$)	0.11 ± 0.02 ($N = 7$)	Swimming
	0.18 ± 0.03 ($N = 7$)	0.24 ± 0.03 ($N = 8$)**	Attached
Shear angle amplitude (rad)	1.34 ± 0.22 ($N = 6$)	1.08 ± 0.20 ($N = 7$)	Swimming
	1.10 ± 0.21 ($N = 7$)	1.35 ± 0.21 ($N = 8$)*	Attached
Shear angle rate (rad s^{-1})	280 ± 70 ($N = 6$)	214 ± 77 ($N = 7$)	Swimming
	185 ± 64 ($N = 7$)	280 ± 90 ($N = 8$)*	Attached
Propagation velocity (mm s^{-1})	1.09 ± 0.26 ($N = 6$)	1.07 ± 0.31 ($N = 7$)	Swimming
	0.79 ± 0.19 ($N = 7$)	0.85 ± 0.26 ($N = 8$)	Attached
Wavelength (μm)	32.6 ± 2.3 ($N = 6$)	34.2 ± 4.5 ($N = 7$)	Swimming
	29.8 ± 3.2 ($N = 7$)	25.7 ± 4.5 ($N = 8$)	Attached

Values are means ± SD (N is the number of spermatozoa).
[a]The solution P15 is ASW, which contains 1 μmol l^{-1} P15.
[b]Flagellar bending is analysed under different mechanical conditions: 'Swimming', in which the spermatozoon swims close to the cover glass or 'Attached', in which it is attached to the cover glass surface by the head.
*Significant at $p < 0.05$ or ** $p < 0.01$ (Student's t-test).
Individual variables are computed using equations (1) to (4) in the text; the curvature and shear angle are determined at 15 μm from the base. Temperature 20 °C.

The amplitude of the shear angle, $\phi_a(s)$, varied with s to a great extent when measured with respect to the head axis, with a peak at half wavelength from the base and a valley at one wavelength, just as observed in sperm of various species (Hiramoto & Baba, 1979; Brokaw, 1979, 1991, 1993), while $\phi_a^x(s)$, the shear angle measured with respect to the x-axis, remained less variable with s either in ASW as demonstrated by Hiramoto & Baba (1979) or in P15. $\phi_a(s)$ had a smaller difference between the peak and the valley in P15 than in ASW. $\phi_a(s)$ at $s = 15$ μm (close to half wavelength) was smaller by 20% in P15 than in ASW, while there was a smaller difference in $\phi^x{}_a(s)$ at $s = 15$ μm between P15 and ASW (Table 2). The shear angle rate at $s = 15$ μm calculated from ϕ of sperm was also lower in P15 than in ASW, while there was a smaller difference in the rate from ϕ^x (Table 2).

Sperm firmly attached by the head

The beat frequency was lower by some 20% in attached sperm than those that were swimming in ASW, while

https://doi.org/10.1017/S0967199405003503 Published online by Cambridge University Press

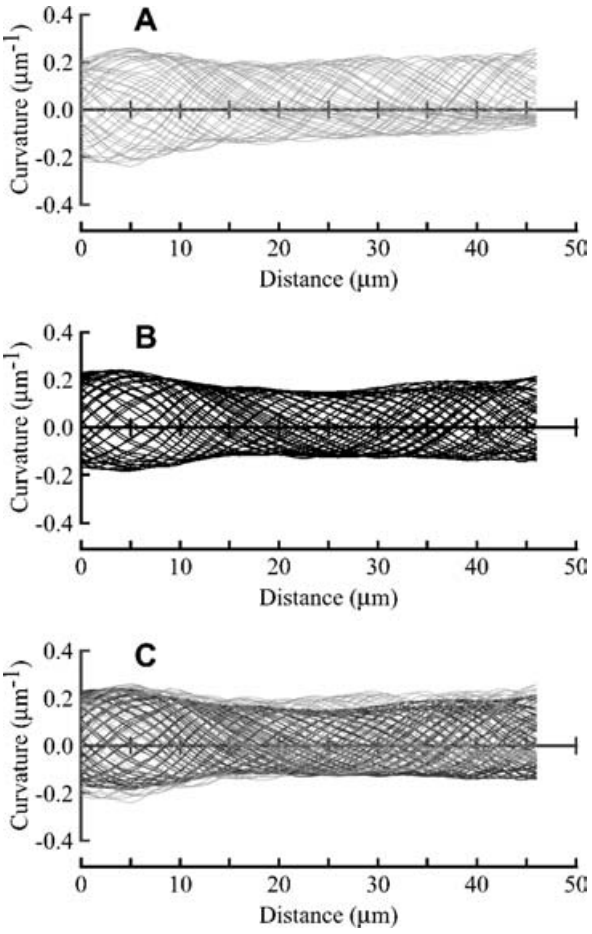


Figure 2 P15-induced changes in flagellar bending of *Aphelasterias japonica* sperm. The curvature of a bending flagellum against the distance measured along the flagellum from the base (1 μm division) is plotted for sperm in ASW (*A*), in 1 μmol l^{-1} P15 (*B*) and superimposed for comparison (*C*). Fifty successive waveforms from a 1000-fps HSVTR are shown with the principal bend having a plus sign. Temperature 20 °C.

it recovered to the same level when sperm were placed in P15 if attached by the head to the solid surface (Table 2). There was a striking increase in the curvature of flagellar bending either in the P bend or in the R bend of sperm in P15 compared with those in ASW (Fig. 3; Table 2). The increment was some 40% at 15 μm (Table 2) and the increase was found overall from base to tip (Fig. 3). The beating of attached sperm in P15 was highly symmetrical over the entire length of the flagellum compared with those either attached in ASW or swimming in P15 (Figs. 1, 3). The propagation velocity of the bending wave was slightly lower in attached sperm than those that were swimming because of a reduction in the beat frequency and wavelength in attached sperm (Table 2), while the flagellar shaft of attached sperm in ASW swung as rapidly as that of sperm swimming in ASW and the swing was even more vigorous in attached sperm in P15 than in ASW (Table 2). The curvature and shear angle of flagella changed sinusoidally as functions of time; data points of $\phi(s, t)$ and those of $\gamma(s, t)$ and respective curves fitted using equations (1) and (3) are shown for measurements at 15 μm from the base in Fig. 4A, B. For measurements taken at all points along the flagellum at 2.5 μm intervals the goodness of fit was tolerably high to an extent similar to that seen in these graphs, giving graphs of a profile of the amplitude $\phi_a(s)$ (Fig. 4C) and $\gamma_a(s)$ demonstrated by the change in the curvature of flagellar waveform as shown in Fig. 3. The amplitude of shear angle, $\phi_a(s)$, increased by 35% on average at 15 μm (Table 2) and often up to 0.5π (right angle to the wave axis) in P15, a much larger angle than in ASW (Fig. 4C). The phase angle appeared to be a linear function of s and allowed a reliable analysis by equations (2) and (4): data points and a line fitted by the method of least squares are shown in Fig. 4D for $S_\phi(s)$ and those for $S_\gamma(s)$ are omitted because of limited space. The wavelength determined from the slope of this fitted line remained rather constant over a wide range from base to tip and is therefore presented as a value not specified for a particular distance from the base (Table 2). The wavelength was slightly shorter in P15 than in ASW (Fig. 4D; Table 2).

Discussion

In a three-dimensional space in seawater, starfish spermatozoa swim along helical paths of, on average, 84 μm pitch and 24.8 μm diameter at a speed of 259 μm s^{-1} (Hiramoto & Baba, 1978), that is, sperm swim at a speed of 176 μm s^{-1} in the direction of the helical axis, calculated by a geometrical equation of helices (Gray, 1955; Crenshaw, 1990). At this 'locomotion' speed, it will take a minimum of about a minute for sperm to move only 10 mm. It is therefore not surprising that sperm can retain for several minutes the ability to respond to asterosap by modulating their flagellar movement, as found in the present study. It has been demonstrated that asterosap-induced rises in $[cGMP]_i$ and $[Ca^{2+}]_i$ are maintained at a relatively high level during a period of observation of up to 20 s at least (Matsumoto *et al.*, 2003).

There have been a couple of proposals for a model of the sperm chemotaxis mechanism based on the sperm response to chemical concentration gradients (Cook *et al.*, 1994; Ishikawa *et al.*, 2004). It has been demonstrated that the gradient of attractant plays an essential role in attracting abalone sperm to an egg (Riffell *et al.*, 2002, 2004). Cook *et al.* (1994) estimated that a diffusional gradient of speract

https://doi.org/10.1017/S0967199405003503 Published online by Cambridge University Press

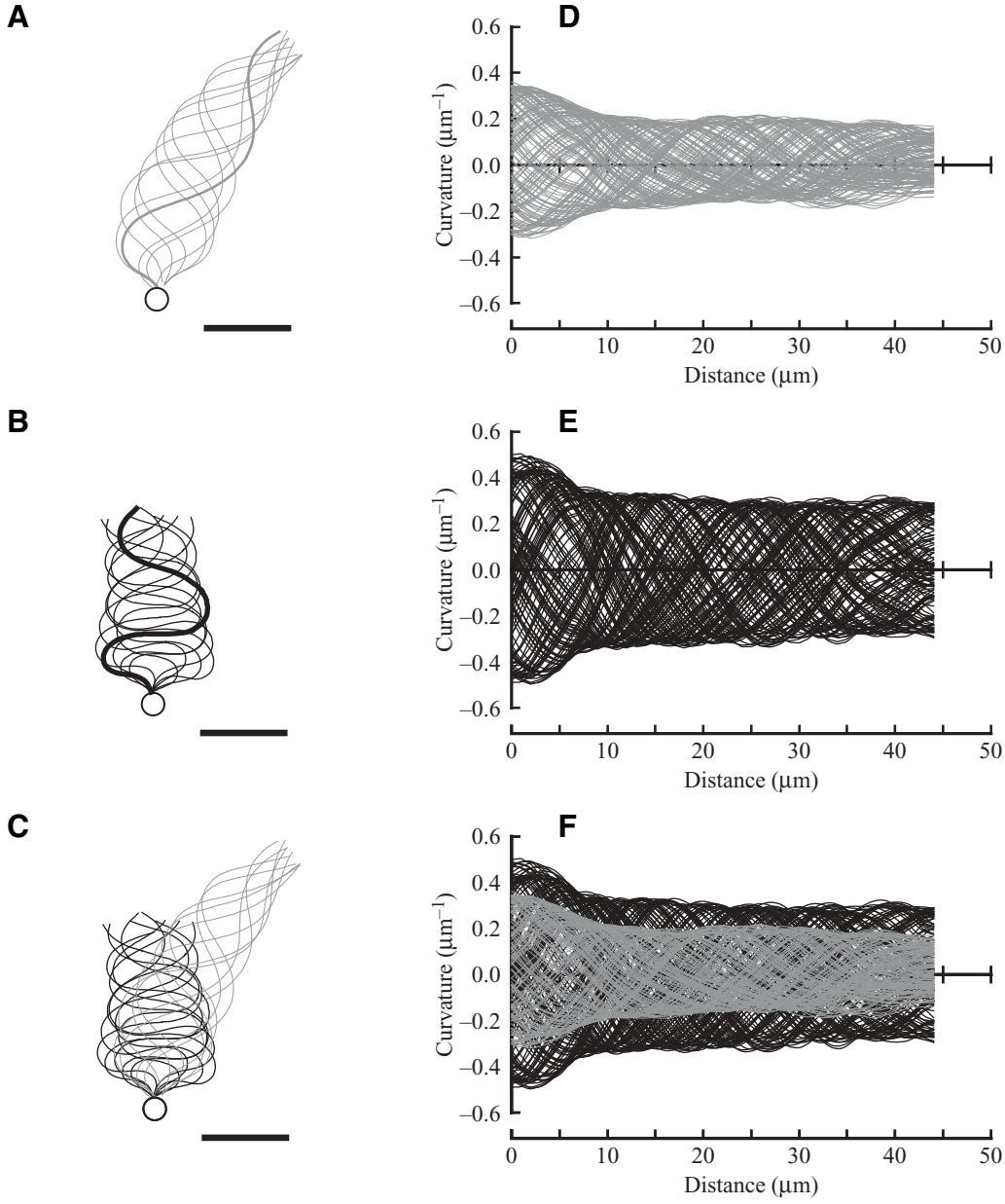


Figure 3 P15-induced changes in bending forms of *Aphelasterias japonica* sperm attached by the head. (*A*)–(*C*) Bending forms from a VTR of sperm in ASW (*A*), in 1 μmol l^{-1} P15 (*B*) and superimposed for comparison (*C*). The curvature against the distance from the base (1 μm division) is plotted for sperm in ASW (*D*), in 1 μmol l^{-1} P15 (*E*) and superimposed for comparison (*F*). Ten bending forms with one highlighted at the same phase in (*A*) and (*B*), respectively, and 150 waveforms in (*D*) and (*E*) are shown. Scale bars represent 10 μm. Temperature 20 °C.

spanning the picomolar to micromolar response range is established over a spherical radius of the order of 1 mm around the egg. Ishikawa *et al*. (2004) obtained a diffusional gradient of the same scale at 60 s in computer simulation of two-dimensional diffusion of a substance with an appropriate diffusional coefficient. The profile of a diffusional gradient depends on boundary conditions and varies with time unless under steady-state conditions, but it is generally a bell-shaped curve (Crank, 1975). It could therefore be safely assumed that asterosap concentration is higher and of a less steep gradient in the region closer to the egg. Thus, our findings about the behaviour of sperm in P15 at concentrations as high as 1 μmol l^{-1} will represent that of sperm just approaching the egg. Straight swimming with a symmetrical flagellar beat enables sperm to approach the egg with an incident angle suitable for the acrosome reaction (Fig. 5A, left) if they are appropriately oriented at earlier stages of chemoattraction as argued by Cook *et al*.

https://doi.org/10.1017/S0967199405003503 Published online by Cambridge University Press

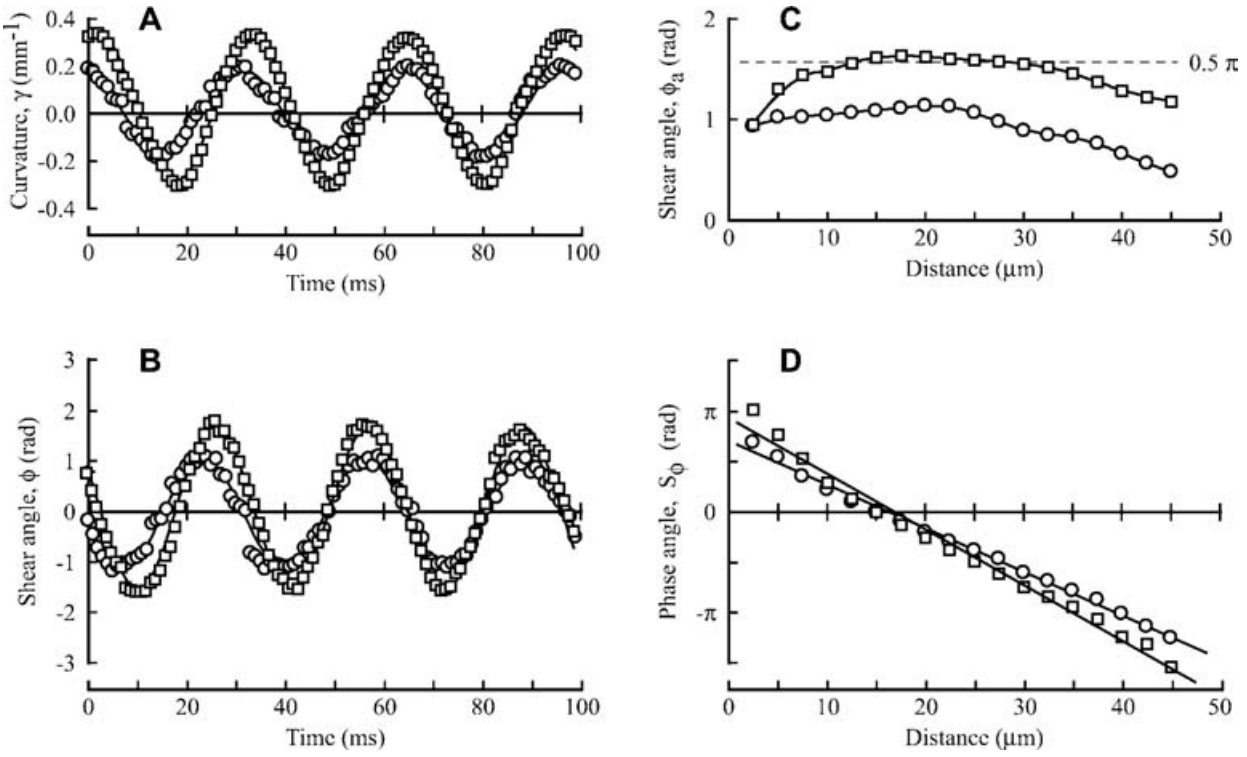


Figure 4 P15-induced changes in the curvature and shear angle of *Aphelasterias japonica* sperm attached by the head. (*A*) The curvature at 15 μm from the base is plotted against time, i.e. γ ($s = 15$, t), for sperm in ASW (open circles) and in 1 μmol l^{-1} P15 (open rectangles) with regression lines (equation (3) in the text). (*B*) The shear angle at 15 μm from the base is plotted against time, i.e. ϕ ($s = 15$, t), for sperm in ASW (open circles) and in 1 μmol l^{-1} P15 (open rectangles) with regression lines (equation (1) in the text). (*C*) The amplitude of shear angle, $\phi_a(s)$, is plotted against the distance from the base for sperm in ASW (open circles) and in 1 μmol l^{-1} P15 (open rectangles). The dashed line indicates amplitude, at which the flagellum must resist most efficiently the force parallel to the wave axis. (*D*) The phase angle is plotted against the distance from the base for sperm in ASW (open circles) and in 1 μmol l^{-1} P15 (open rectangles) with regression lines (equation (2) in the text). Temperature 20 °C.

(1994). In contrast, swimming in a circle with a more asymmetrical flagellar beat causes sperm to approach the egg with an oblique incident angle (Fig. 5B, left), which will lead to a failure of fertilization. A symmetrical flagellar beat will also serve to maintain sperm orientation during the acrosome reaction (Fig. 5A, middle to right) instead of generating a torque that may cause a deviation in the insertion of the acrosomal process (Fig. 5B, middle to right).

The amplitude of the shear angle, $\phi_a(s)$, has a wave-like profile with peaks at $(n+0.5)\lambda_\phi$ and with valleys at $n\lambda_\phi$, where $n = 0$ or 1 and so on (Hiramoto & Baba, 1979; Brokaw, 1979, 1991, 1993). Brokaw (1979, 1991) interpreted this fact as caused by interference between metachronous and synchronous sliding. The reduction in $\phi_a(s)$ at s = 15 μm ($0.5\lambda_\phi$) for swimming sperm in P15 may indicate a reduction in this interference. Irrespective of any changes in metachronous sliding or synchronous sliding, there are no significant differences in $\phi_a^x(s)$ or in the beat frequency, wavelength and propagation velocity of flagellar bending between sperm swimming in ASW and those swimming in P15. This implies a minimum change in the propulsive forces of sperm swimming in P15 because the hydrodynamic drag in the direction of the wave axis largely depends on the angular direction of the flagellar shaft with respect to this axis and also on the beat frequency and wavelength. In fact the swimming velocity is not affected by P15. On the other hand, sperm, when attached in the presence of asterosap, may increase their propulsive forces in the direction of wave axis because the amplitude of $\phi_a^x(s)$ as well as its rate of change is larger in attached sperm in P15 than in those attached in ASW.

To understand the hydrodynamics of the acrosomal process extending into the jelly layer of the starfish oocytes, it is helpful to define the dimensions of these objects. The acrosomal process of starfish sperm is about 25 μm (range 22–28 μm) in length measured by light microscopy and 0.13 μm in diameter measured by electron microscopy (Dan, 1954). Schroeder (1981) reported that a starfish oocyte has a diameter of about 160 μm and the flagellated squamous follicle cells are separated from it by a distance of 10–25 μm, the

https://doi.org/10.1017/S0967199405003503 Published online by Cambridge University Press

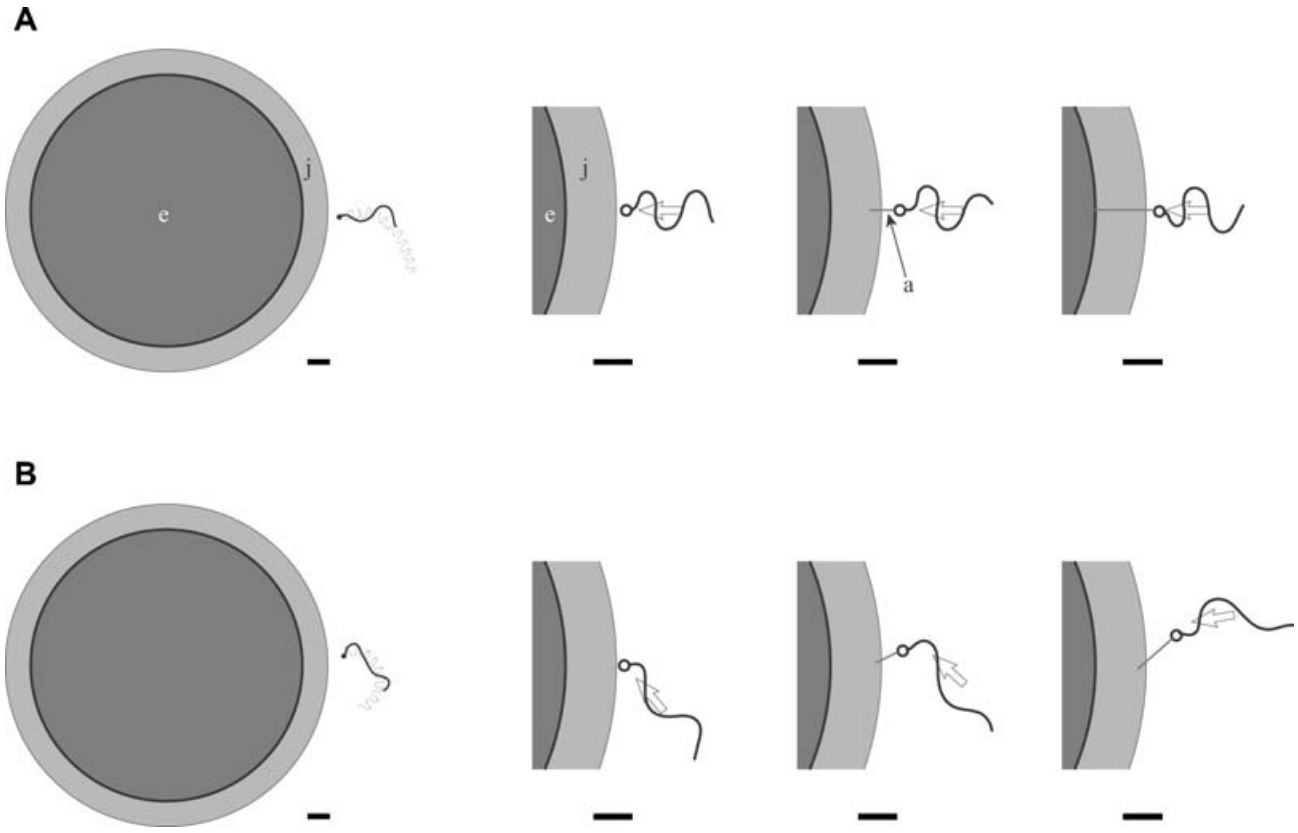


Figure 5 Roles in fertilization of asterosap-induced 'hyperactivation' of starfish sperm. Events are depicted from left to right beginning with the encounter of a spermatozoon with an egg (e), followed by the acrosome reaction of the spermatozoon and ending with successful (*A*) or unsuccessful (*B*) fertilization. 'Hyperactivation' as found in P15, i.e. swimming along a rather straight path and vigorous symmetrical bending upon attachment, may make it more probable that the spermatozoon approaches the jelly layer (j) with the head axis normal to its surface and helps the acrosomal process (a) more steadily to extend toward the membrane (*A*) as compared with a hypothetical control (no 'hyperactivation') in which the spermatozoon kept the flagellar movement unaffected by the egg (*B*). Scale bars represent 10 μm but the thickness of the flagellum and acrosomal process are not drawn to scale.

intervening space being filled with the jelly coat, which gradually swells in seawater and appears flocculent or lightly fibrous in the light microscope. Thus the jelly layer can safely be assumed to be 10–25 μm or more in thickness, though the thickness can only be defined within a wide range because of the layer's amorphousness. Briefly, the acrosomal process has a length sufficient to reach the oocyte surface membrane provided that the sperm is firmly anchored by the head, the tip of which can be bound to the ARIS on the jelly layer surface (Kawamura *et al*., 2002; Longo *et al*., 1995; Ushiyama *et al*., 1993). The resistance of a cylinder moving through a fluid in the direction of the major axis of the cylinder is given by

$$F = 4\pi\mu Ua/(\ln(2a/b) - 0.72) \quad (5)$$

where μ, U, a and b are the viscosity of the fluid, the velocity, and the half length and radius of the cylinder (Happel & Brenner, 1986). The resistance is also expressed by

$$F = 6\pi\mu UR \quad (6)$$

where R is the Stokes' radius of a hydrodynamically equivalent sphere (Happel & Brenner, 1986). From equations (5) and (6), R is given by

$$R = l/(3(\ln(2l/c) - 0.72)) \quad (7)$$

where $l = 2a$ and $c = 2b$ are the length and diameter of the cylinder, respectively. Taking $l = 25$ μm and $c = 0.13$ μm for evaluation of the resistance to a cylinder, which is assumed to be hydrodynamically equivalent to the acrosomal process in the fully extended state, we get $R = 1.6$ μm, which is a little larger than the radius of the starfish sperm head, 1.2 μm (Hiramoto & Baba, 1978). This means that a spermatozoon with the acrosomal process growing into the jelly layer will encounter a substantial viscous resistance as well. The viscous resistance also depends on the speed of elongation of the acrosomal process and the viscosity of the jelly

https://doi.org/10.1017/S0967199405003503 Published online by Cambridge University Press

coat. The elongation speed has been measured with *Thyone* sperm, in which the data plotted as (length)^2 versus time are linear and the rate of elongation is 330–960 $\mu m^2\ s^{-1}$ (Tilney & Inoué, 1982, 1984). This relationship is expressed by

$$x^2 = a(t + \beta) \tag{8}$$

where x, t, a and β are the length of the process, time, and the rate and initial lag time of elongation, respectively. By differentiating equation (8) we get

$$dx/dt = 0.5a/x \tag{9}$$

where dx/dt is the elongation speed. The elongation speed at $x = 10\,\mu m$, for example, is some $30\,\mu m\,s^{-1}$, taking the median value of the rate of elongation of *Thyone* sperm described above. Although this value is about one-tenth of the swimming velocity of sperm in seawater, the resistance of the acrosomal process extending in the jelly layer can be substantial because the jelly coat of echinoderm eggs has a composite structure of irregularly arranged fibrous networks embedded in a jelly matrix and the viscosity of the matrix is probably much higher than that of seawater (Thomas *et al*., 2001). The vigorous flagellar movement in the 'hyperactivated' state produced by asterosap, as found in the present study, would serve for sperm to extend the acrosomal process into the jelly layer by increasing propulsive forces in the direction of process elongation, which will take place in the direction of the wave axis when the flagellar movement is symmetrical, and by enhancing hydrodynamic resistances to the backlash from the advancing process (Fig. 5); it should be noted in this context that the resistance to the backlash is maximized when the flagellar shaft is perpendicular to the backward-pushing force (Gray, 1955; Hiramoto & Baba, 1978). This may greatly help the acrosome reaction, as well as firm binding of the head tip to the ARIS (Kawamura *et al*., 2002; Longo *et al*., 1995; Ushiyama *et al*., 1993) and symmetrical flagellar movement as found in the present study.

It has been demonstrated by various investigators (Brokaw & Gibbons, 1975; Hiramoto & Baba, 1978; Ishijima & Hiramoto, 1994) and is confirmed in the present study (Table 2) that various mechanical conditions, such as whether the head is free or fixed, may significantly change the flagellar waveform and the beat frequency. Our findings (Figs. 3, 4; Table 2) indicate that this load-dependent modification of the flagellar bending in free swimming or attached sperm can be affected by the axonemal state induced by asterosap. It is likely that the 'hyperactivated' state may be induced by asterosap through changes in $[Ca^{2+}]_i$, pH_i or $[cAMP]_i$, which are occur via the cGMP-signalling pathway (Hoshi *et al*., 1994, Nishigaki *et al*., 2004; Matsumoto *et al*., 2003; Eisenbach, 2004). The study of molecular mechanisms of this sort of modulation may deepen our understanding of flagellar movement.

References

Baba, S.A. & Mogami, Y. (1985). An approach to digital image analysis of bending shapes of eukaryotic flagella and cilia. *Cell Motil*. **5**, 475–89.

Baba, S.A. & Mogami, Y. (1987). Device for controlled intensification of the light output of xenon flash tubes. *Rev. Sci. Instrum*. **58**, 1312–13.

Bevington, P.R. & Robinson, D. (1992). *Data Reduction and Error Analysis for the Physical Sciences*, 2nd edn. New York: McGraw-Hill.

Böhmer, M., Van, Q., Weyand, I., Hagen, V., Beyermann, M., Matsumoto, M., Hoshi, M., Hildebrand, E. & Kaupp, U.B. (2005). Ca^{2+} spikes in the flagellum control chemotactic behavior of sperm. *EMBO J*. **24**, 2741–52.

Brokaw, C.J. (1979). Calcium-induced asymmetrical beating of Triton-demembranated sea urchin sperm flagella. *J. Cell Biol*. **82**, 401–11.

Brokaw, C.J. (1991). Microtubule sliding in swimming sperm flagella: direct and indirect measurements on sea urchin and tunicate spermatozoa. *J. Cell Biol*. **165**, 1201–5.

Brokaw, C.J. (1993). Microtubule sliding in reduced-amplitude bending waves of *Ciona* sperm flagella: resolution of metachronous and synchronous sliding components of stable bending waves. *Cell Motil. Cytoskeleton* **26**, 144–62.

Brokaw, C.J. & Gibbons, I.R. (1975). Mechanisms of movement in flagella and cilia. In *Swimming and Flying in Nature* (ed. T.W.-T. Wu, C.J. Brokaw & C. Brennen), pp. 89–126. London and New York: Academic Press.

Cook, S.P., Brokaw, C.J., Muller, C.H. & Babcock, D.F. (1994). Sperm chemotaxis: egg peptides control cytosolic calcium to regulate flagellar responses. *Dev. Biol*. **114**, 1201–19.

Cosson, M.P., Carre, D. & Cosson, J. (1984). Sperm chemotaxis in siphonophores. II. Calcium-dependent asymmetrical movement of spermatozoa induced by the attractant. *J. Cell Sci*. **68**, 163–81.

Crank, J. (1975). *The Mathematics of Diffusion*, 2nd edn. Oxford: Clarendon Press.

Crenshaw, H.C. (1990). Helical orientation – a novel mechanism for the orientation of microorganisms. *Lecture Notes Biomath*. **89**, 361–86.

Dan, J.C. (1952). Studies on the acrosome. I. Reaction to egg-water and other stimuli. *Biol. Bull*. **99**, 54–66.

Dan, J.C. (1954). Studies on the acrosome. II. Acrosome reaction in starfish spermatozoa. *Biol. Bull*. **107**, 203–18.

Darszon, A., Labarca, P., Nishigaki, T. & Espinosa, F. (1999). Ion channels in sperm physiology. *Physiol. Rev*. **79**, 481–510.

Eisenbach, M. (1999). Sperm chemotaxis. *Dev. Reprod*. **4**, 56–66.

Eisenbach, M. (2004). Towards understanding the molecular mechanism of sperm chemotaxis. *J. Gen. Physiol*. **124**, 105–8.

Gray, J. (1955). The movement of sea-urchin spermatozoa. *J. Exp. Biol*. **32**, 775–801.

Happel, J. & Brenner, H. (1986). *Low Reynolds Number Hydrodynamics*, 4th edn. Dordrecht: Martinus Nijhoff.

https://doi.org/10.1017/S0967199405003503 Published online by Cambridge University Press

Hiramoto, Y. & Baba, S.A. (1978). A quantitative analysis of flagellar movement in echinoderm spermatozoa. *J. Exp. Biol*. **76**, 85–108.

Hoshi, M., Nishigaki, T., Ushiyama, A., Okinaga, T., Chiba, K. & Matsumoto, M. (1994). Egg-jelly signal molecules for triggering the acrosome reaction in starfish spermatozoa. *Int. J. Dev. Biol*. **38**, 167–74.

Ishijima, S. & Hiramoto, Y. (1994). Flexural rigidity of echinoderm sperm flagella. *Cell Struct. Funct*. **19**, 349–62.

Ishikawa, M., Tsutsui, H., Cosson, J., Oka, Y. & Morisawa, M. (2004). Strategies for sperm chemotaxis in the siphonophores and ascidians: a numerical simulation study. *Biol. Bull*. **206**, 95–102.

Kaupp, U.B., Solzin, J., Hildebrand, E., Brown, J.E., Helbig, A., Hagen, V., Beyermann, M., Pampaloni, F. & Weyand, I. (2003). The signal flow and motor response controling chemotaxis of sea urchin sperm. *Nat. Cell Biol*. **5**, 109–17.

Kawamura, M., Matsumoto, M. & Hoshi, M. (2002). Characterization of the sperm receptor for acrosome reaction-inducing substance of the starfish. *Asterias amurensis*. *Zool. Sci*. **19**, 435–42.

Longo, F.J., Ushiyama, A., Chiba, K. & Hoshi, M. (1995). Ultrastructural localization of acrosome reaction-inducing substance (ARIS) on sperm of the starfish. *Asterias amurensis*. *Mol. Reprod. Dev*. **41**, 91–9.

Matsumoto, M., Briones, A.V., Nishigaki, T. & Hoshi, M. (1999). Sequence analysis of cDNAs encoding precursors of starfish asterosaps. *Dev. Genet*. **25**, 130–6.

Matsumoto, M., Ikeda, M. & Hoshi, M. (2000). Sperm-specificity of the acrosome reaction in starfish. *Zygote* **8**, S62.

Matsumoto, M., Solzin, J., Helbig, A., Hagen, V., Ueno, S., Kawase, O., Maruyama, Y., Ogiso, M., Godde, M., Minakata, H., Kaupp, U.B., Hoshi, M. & Weyand, I. (2003). A sperm-activating peptide controls a cGMP-signaling pathway in starfish sperm. *Dev. Biol*. **260**, 314–24.

Miller, R.L. & Vogt, R. (1996). An N-terminal partial sequence of the 13 kDa *Pycnopodia helianthoides* sperm chemoattractant 'startrak' possesses sperm-activating activity. *J. Exp. Biol*. **199**, 311–18.

Miyake, M.O., Mogami, Y., Kataoka, E., Kajita, E. & Baba, S.A. (1998). Improvement in time and space resolution of stroboscopic micrography using high power xenon flash. *Rev. Sci. Instrum*. **69**, 325–6.

Nishigaki, T., Chiba, K., Miki, W. & Hoshi, M. (1996). Structure and function of asterosaps, sperm-activating peptides from the jelly coat of starfish eggs. *Zygote* **4,** 237–45.

Nishigaki, T., Chiba, K. & Hoshi, M. (2000). A 130-kDa membrane protein of sperm flagella is the receptor for asterosaps, sperm-activating peptides of starfish. *Asterias amurensis*. *Dev. Biol*. **219**, 154–62.

Nishigaki, T., Wood, C.D., Tatsu, Y., Yumoto, N., Furuta, T., Elias, D., Shiba, K., Baba, S.A. & Darszon, A. (2004). A sea urchin egg jelly peptide induces a cGMP-mediated decrease in sperm intracellular Ca^{2+} before its increase. *Dev. Biol*. **272**, 376–88.

Ohmuro, J., Mogami, Y. & Baba, S.A. (2004). Progression of flagellar stages during artificially delayed motility initiation in sea urchin sperm. *Zool. Sci*. **21**, 1099–108.

Riffell, J.A., Krug, P.J. & Zimmer, R.K. (2002). Fertilization in the sea: the chemical identity of an abalone sperm attractant. *J. Exp. Biol*. **205**, 1439–50.

Riffell, J.A., Krug, P.J. & Zimmer, R.K. (2004). The ecological and evolutionary consequences of sperm chemoattraction. *Proc. Natl. Acad. Sci. USA* **101**, 4501–6.

Schroeder, T.E. (1981). Mcrofilament-mediated surface change in starfish oocytes in response to 1-methyladenine: implications for identifying the pathway and receptor sites for maturation-inducing hormones. *J. Cell Biol*. **90**, 362–71.

Shiba, K., Mogami, Y. & Baba, S.A. (2002). Ciliary movement in sea-urchin embryos. *Natural Science Report, Ochanomizu University* **53**, 49–54.

Shiba, K., Ohmuro J., Mogami, Y., Nishigaki T., Wood, C.D., Darszon, A., Tatsu, Y., Yumoto, N. & Baba, S.A. (2005). Sperm-activating peptide induces asymmetric flagellar bending in sea urchin sperm. *Zool. Sci*. **22**, 293–9.

Thomas, F., Bolton, T. & Sastry, A. (2001). Mechanical forces imposed on echinoid eggs during spawning: mitigation of forces by fibrous networks within egg extracellular layers. *J. Exp. Biol*. **204**, 815–21.

Tilney, L.G. & Inoué, S. (1982). Acrosomal reaction of *Thyone* sperm. II. The kinetics and possible mechanism of acrosomal process elongation. *J. Cell Biol*. **93**, 820–7.

Tilney, L.G. & Inoué, S. (1985). Acrosomal reaction of the *Thyone* sperm. III. The relationship between actin assembly and water influx during the extension of the acrosomal process. *J. Cell Biol*. **100**, 1273–83.

Ushiyama, A., Araki, T., Chiba, K. & Hoshi, M. (1993). Specific binding of acrosome-reaction-inducing substance to the head of starfish spermatozoa. *Zygote* **1**, 121–7.

Ward, G.E., Brokaw, C.J., Garbers, D.L. & Vacquier, V.D. (1985). Chemotaxis of *Arbacia punctulata* spermatozoa to resact, a peptide from the egg jelly layer. *J. Cell Biol*. **101**, 2324–9.

Yoshida, M., Ishikawa, M., Izumi, H., De Santis, R. & Morisawa, M. (2003). Store-operated calcium channel regulates the chemotactic behavior of ascidian sperm. *Proc. Natl. Acad. Sci. USA* **100**, 149–54.

https://doi.org/10.1017/S0967199405003503 Published online by Cambridge University Press